Available online at www.sciencedirect.com
ScienceDirect
Journal of Power Sources 159 (2006) 34–37
JOURNAL OF POWER SOURCES
www.elsevier.com/locate/jpowsour

Short communication

Fe-based amorphous alloys as bipolar plates for PEM fuel cell

E. Fleury [a], J. Jayaraj [b], Y.C. Kim [a], H.K. Seok [a], K.Y. Kim [a], K.B. Kim [a,*]

[a] *KIST, Advanced Metals Research Center, Seoul, Republic of Korea*
[b] *International R&D Academy, KIST-University of Science and Technology, Seoul, Republic of Korea*

Available online 16 June 2006

Abstract

Two compositions of Fe-based $Fe_{50}Cr_{18}Mo_8Al_2Y_2C_{14}B_6$ and $Fe_{44}Cr_{15}Mo_{14}Y_2C_{15}B_6N_4$ amorphous alloys were developed as alternative bipolar plate material for polymer electrolyte membrane fuel cell (PEMFC). In this paper, we present results of an investigation on the electrical, mechanical, corrosion properties and processing ability of these amorphous alloys. The combination of excellent properties indicated that Fe-based amorphous alloys could be potential candidate materials as bipolar plates in PEMFC.

Keywords: Amorphous material; Bipolar plate; Corrosion resistance; Passive layer

1. Introduction

It is desirable to produce bipolar plates for polymer electrolyte membrane fuel cell (PEMFC) as thin as possible, to replace the bulky graphite bipolar plates, in order to increase the volumetric power density. Intensive researches were thus carried on with the aim of developing alternative materials and, for example graphite composite [1], stainless steel [2], and TiN coating deposited on metallic substrate were recently proposed [3]. Considering the requirements for bipolar plate, further enhancement of the corrosion properties is however required for metallic bipolar plates. We previously introduced a novel idea of using metallic amorphous materials [4] as bipolar plates from the corrosion stand point. In this paper, besides the corrosion properties of two Fe-based amorphous alloys evaluated in simulated PEMFC environment, other properties such as contact resistance, mechanical and viscosity properties are presented. The potential of the $Fe_{50}Cr_{18}Mo_8Al_2Y_2C_{14}B_6$ and $Fe_{44}Cr_{15}Mo_{14}Y_2C_{15}B_6N_4$ amorphous alloys for bipolar plate applications in PEMFC are discussed.

2. Experimental procedure

$Fe_{50}Cr_{18}Mo_8Al_2Y_2C_{14}B_6$ and $Fe_{41}Cr_{18}Mo_{14}Y_2C_{15}B_6N_4$ (at.%) alloy compositions were prepared by arc melting high purity metal, Fe (99.9%), Cr (99.9%), Mo (99.5%), Al (99.9%), Y (99.5%), C (99.9%), B (99.9%) and Fe–Cr–N master alloy, under an argon atmosphere. Sample plates of dimension 1.2 mm × 5 mm × 50 mm were prepared by copper mold casting. The microstructural characterization of the plates was performed by X-ray diffraction (XRD) with monochromatic Cu Kα radiation and transmission electron microscopy (TEM). A method explained elsewhere [5] was used to measure the contact resistance of the alloys with the specimen thickness of 1.1 mm and a cross-section area of 0.7 cm^2. To investigate the surface energy of the samples, the water contact angle was measured by "CAM + contact angle meter". The density of the samples was measured according to the ASTM D792 test procedure. The fracture strength of the amorphous alloys were obtained by performing uniaxial compression tests on a cast cylindrical specimens of 2 mm diameter and 4 mm height at room temperature on an Instron-type machine with an initial strain rate of 1×10^{-4} s^{-1}. The corrosion behavior of the amorphous plates was studied by electrochemical measurements in a simulated aggressive PEMFC environment; all the experiments were conducted in 1 M H_2SO_4 + 2 ppm F^- at 80 °C [6,7] under either hydrogen gas or pressurized air bubbled into the solution throughout the experiments to simulate the respective anodic and cathodic PEMFC environments, as described by Jayaraj et

* Corresponding author at: Korea Institute of Science and Technology, Division of Materials Science, P.O. Box 131, Cheongryang, Seoul 130-650, Republic of Korea. Tel.: +82 2 958 5454; fax: +82 2 958 5449.
E-mail address: kibaekim@kist.re.kr (K.B. Kim).

0378-7753/$ – see front matter © 2006 Elsevier B.V. All rights reserved.
doi:10.1016/j.jpowsour.2006.04.119

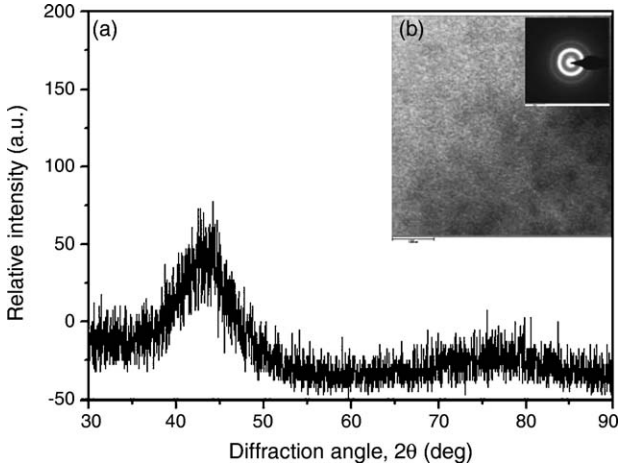

Fig. 1. (a) XRD pattern of $Fe_{41}Cr_{18}Mo_{14}Y_2C_{15}B_6N_4$ cast plate of dimension 1.2 mm × 5 mm × 50 mm showing the amorphous nature; (b) typical dark field TEM image and corresponding SADP.

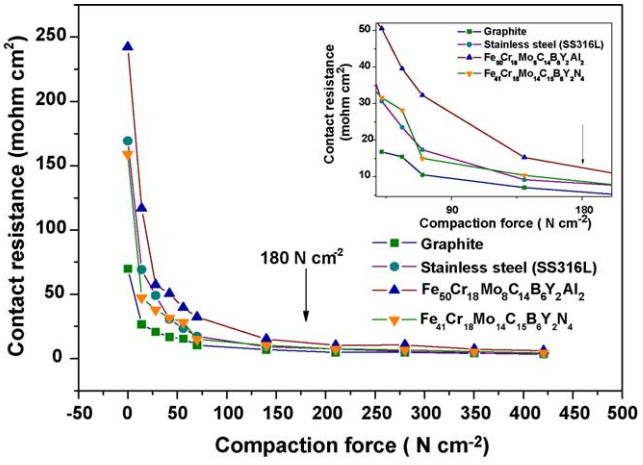

Fig. 2. Contact resistance of graphite, stainless steel and Fe-based amorphous alloys measured at various compaction forces (inset shows details around 180 N cm^{-2}).

al. [4]. The viscosity of the Fe-based amorphous alloys were measured by means of a Perkin-Elmer thermal mechanical analyzer (TMA7) with a quartz penetration probe (Ø 3.7 mm) under argon atmosphere, a static force of 250 mN and a heating rate of 20 °C min^{-1}.

3. Results and discussion

3.1. Microstructural characterization

Fig. 1(a) shows the XRD pattern of the $Fe_{41}Cr_{18}Mo_{14}Y_2C_{15}B_6N_4$ amorphous plate. The broad peak observed for the diffraction angle 2θ ranging between 40° and 50° demonstrates the absence of crystalline phase. The amorphous structure of the plate was further confirmed by TEM analysis. Fig. 1(b) reveals a homogeneous structure without any crystalline phase and the corresponding selected area diffraction pattern (SADP) shows diffuse halo ring characteristics of the amorphous structure.

3.2. Electrical properties

In general, the electrical resistivity of the amorphous alloy is higher than that of its crystalline state because of the reduced mobility of the conduction electrons in the amorphous state. Fe-based amorphous alloy exhibits an electrical resistivity of the order of 100–130 μΩ cm at room temperature [8] which is slightly larger than the values for stainless steel. However, the contact resistance has a stronger influence on the cell performance than the bulk resistance of the bipolar plate [5]. The contact resistance, which includes the bulk resistance of the bipolar plate material and two gas diffusion layers, as well as the interfacial resistance between the plate and the gas diffusion layers, was measured as a function of the compaction force. The contact resistance decreased with the increasing compaction force as shown in Fig. 2, which can be explained by the decrease of the interfacial resistance. At a given compaction force the contact resistance of $Fe_{41}Cr_{18}Mo_{14}Y_2C_{15}B_6N_4$ was lower than that of the $Fe_{50}Cr_{18}Mo_8Al_2Y_2C_{14}B_6$ amorphous alloy similar to SS316L, however, higher than that of graphite. At stack assembly condition, i.e., about 180 N cm^{-2}, the difference between the contact resistance of the amorphous alloys to the stainless steel and graphite is negligible indicating that these Fe-based amorphous alloys can be applied as bipolar plates for PEMFC from the stand point of electrical properties.

3.3. Physical properties

In addition to electrical properties the bipolar plate material requires gas tightness, low water absorption, sufficient mechanical strength, low weight and chemical stability in the PEMFC environment. The water absorption at the cathodic part of the bipolar plate, which depends on the wettability of the material, affects the cell performance [5]. The surface energy of the Al- and N-containing Fe-based amorphous alloy was obtained by measuring the wetting angle (θ) and values are given in Table 1. Values of the surface energy for amorphous alloys are higher than that of stainless steel (76°) but lower than that of graphite (104°). Although, not as efficiently as graphite, it can be predicted that the water produced in PEMFC can flow and be easily removed when on contact with Fe-based amorphous bipolar plate.

Values of the fracture strength (σ_f) and density (ρ) of Fe-based amorphous are given in Table 1. The measured densities

Table 1
Properties of Fe-based amorphous alloy

Alloy	T_g (°C)	T_{x1} (°C)	T_{x2} (°C)	σ_f (MPa)	ρ (g cm^{-3})	θ (°)
$Fe_{50}Cr_{18}Mo_8Al_2Y_2C_{14}B_6$	560	606	669	3617	7.48	92
$Fe_{41}Cr_{18}Mo_{14}Y_2C_{14}B_6N_4$	618	656	677	3203	7.75	88

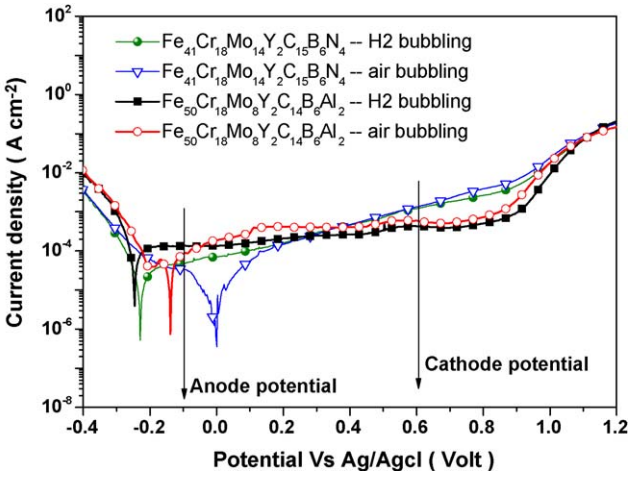

Fig. 3. Potentiodynamic behavior of Fe-based amorphous alloys in 1 M H_2SO_4 + 2 ppm F^- at 80 °C. The anodic and cathodic potential in PEMFC is marked.

of the amorphous alloys are similar to that of stainless steel while the strength of these compositions are approximately 3–4 times larger. The high values of the mechanical properties can also be used advantageously since it allows a reduction of bipolar plate thickness below 1 mm, while still providing high mechanical performance.

3.4. Corrosion behavior of Fe-based amorphous alloys

The polarization curves for the Fe-based amorphous materials in 1 M H_2SO_4 + 2 ppm F^- at 80 °C with hydrogen and air bubbling are shown in Fig. 3. Under hydrogen bubbling, Fe-based amorphous alloys with Al and N passivated spontaneously with a current density, I_{pass}, of the order of 0.133 and 0.031 mA cm^{-2}, respectively, at the approximate operating potential of the PEMFC anodic environment of −0.1 V. The corrosion current density, I_{corr}, was estimated by the Tafel slope method [9] from the potentiodynamic curves. The I_{corr} values for N- and Al-containing alloys were about 36 and 182 μA cm^{-2}, respectively. Thus from the values of I_{pass} and I_{corr}, the N-containing amorphous alloy displays higher corrosion resistance than the Al-containing amorphous alloy in PEMFC anodic environment. Under air bubbling, the I_{pass} is in the order of 0.57 and 1.41 mA cm^{-2} for the Al- and N-containing Fe-based amorphous alloys, respectively, at the approximate operating potential of the PEMFC cathodic environment of 0.6 V. The I_{corr} value of Al-containing alloy in air bubbling was about 0.1 mA cm^{-2} and a very low value of about 5 μA cm^{-2} was obtained for N-containing alloy indicating a higher corrosion resistance of this amorphous alloy in the PEMFC cathodic environment. In comparison to the hydrogen bubbled environment, the lower I_{corr} value in air bubbled environment reflects the useful effect of the air (i.e., oxygen) on the formation of the passive layer. The corrosion potential, E_{corr} of the Al- and N-containing amorphous alloys in H_2 bubbling conditions were −0.247 and −0.229 V, respectively. These corresponding alloys became noble in air bubbling with an E_{corr} value of −0.139 and 0.007 V, indicating that for these compositions H_2 bubbling was more aggressive than air bubbling. Also, the Fe-based amorphous alloy show better corrosion resistance than the stainless steel SS316L in the PEMFC environment [4]. The existence of chemical heterogeneity in the crystalline alloy (stainless steel) prevents the formation of the uniform passive film and the grain boundaries act as potential sites for preferential dissolution to occur, resulting in a higher corrosion rate [10]. Whereas, the corrosion mechanism of this Al-containing Fe-based amorphous alloy was explained by the formation of uniform and thin Cr-rich oxide layer [4]. The effect of N on the corrosion resistance in PEMFC environment has not been elucidated, yet. However, analyses by means of XPS for the passive layer formed in HCl solution were recently reported for N-containing Fe-based amorphous alloy [11]. The presence of N element in the alloy was found to result in the form of nitrides on the outer surface of the passive layer which are negatively charged, like MoN^-. In addition to the Cr-oxide enrichment, the negatively charged N will repel the Cl^- ions of the HCl solution [11], which would result in an enhanced corrosion resistance. Similarly, this mechanism is believed to take place in solution simulating PEMFC environment with the repulsion of SO_4^- and F^- and investigations by means of XPS technique are currently in progress.

3.5. Viscosity

Metallic glassy alloys exhibit a superplastic [12] behavior in the super-cooled liquid region, defined as the temperature range between the glass transition (T_g) and crystallization temperature (T_x). The superplastic behavior of the amorphous alloys in the super-cooled liquid region can be used advantageously [12,13] to process the required flow channels in the bipolar plate at relatively low temperature by metal processing technique like stamping.

The viscosity properties of both amorphous alloys are presented in Fig. 4. The initially high values of the viscosity decreased as the temperature increased, and values became

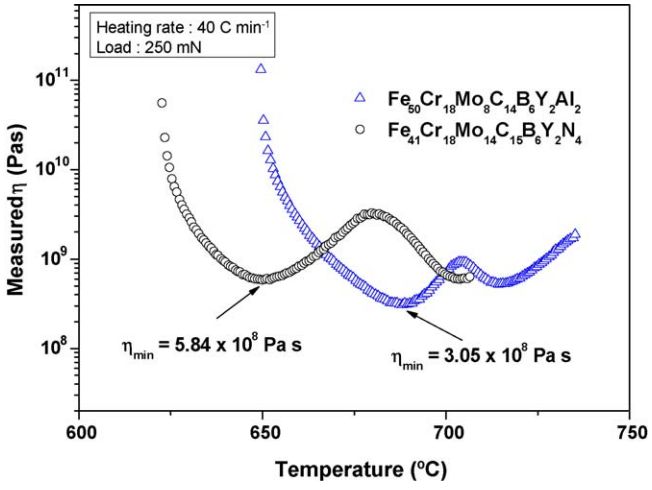

Fig. 4. Measured viscosity of the Fe-based amorphous alloy in the super-cooled liquid region.

particularly low between the T_g and T_x (given in Table 1, obtained from the DSC traces of the amorphous alloy at a heating rate of 20 °C min^{-1}). However, as crystals start to precipitate in the amorphous matrix, the viscosity increased again. The minimum values of the viscosity are about 3×10^{-8} and 5.5×10^{-8} Pa s at 687 and 647 °C for the Al- and N-containing alloys, respectively. Thus, in addition to the larger super-cooled liquid region, the Al-containing alloy displays a lower viscosity than N-containing alloy, suggesting that the Al-containing alloy could be more easily formed in the super-cooled liquid region. Since processing is also an important aspect to take into consideration for the potential of materials for bipolar plates, these data indicated that flow channels can be easily processed in Fe-based amorphous alloys by means of forming technique in the super-cooled liquid region. Recently, Ni-based amorphous bipolar plates have been fabricated by utilizing the superplastic behavior in the super-cooled liquid region [14]. Bipolar plates for PEMFC with the $Fe_{50}Cr_{18}Mo_8Al_2Y_2C_{14}B_6$ and $Fe_{41}Cr_{18}Mo_{14}Y_2C_{15}B_6N_4$ compositions are under construction in the authors' laboratory and will be investigated under real operating conditions.

4. Conclusions

The contact resistances of the Fe-based amorphous alloys were found to be similar to that of stainless steel. These alloys characterized by fracture exhibit strength beyond 3 GPa. These high values of the mechanical properties can be used advantageously since it would allow reduction of bipolar plate thickness below 1 mm. As demonstrated by potentiodynamic studies, both the $Fe_{41}Cr_{18}Mo_{14}Y_2C_{14}B_6N_4$ and $Fe_{50}Cr_{18}Mo_8Al_2Y_2C_{14}B_6$ amorphous alloys exhibit higher corrosion resistances than SS316L. Based on these remarkable properties, Fe-based amorphous alloys appeared as potential candidate materials for bipolar plate in PEMFC.

Acknowledgements

The authors would like to gratefully acknowledge Dr. Eun-Ae Cho and Mr. Mani Prasanna, from the Fuel Cell Research Centre-KIST, for their valuable support. This work was financially supported by KIST research program under contract no. KIST 2E19470 and the Next Generation-New Technology Development Program of Ministry of Commerce, Industry and Energy in Korea under contract no. KIST 2M17190.

References

[1] J. Scholta, B. Rohland, V. Trapp, U. Focken, J. Power Sources 84 (1999) 231–234.
[2] J.S. Kim, W.H.A. Peelen, K. Hemmes, R.C. Makkus, Corros. Sci. 44 (2002) 635–655.
[3] M. Li, S. Luo, C. Zeng, J. Shen, H. Lin, C. Cao, Corros. Sci. 46 (2004) 1369–1380.
[4] J. Jayaraj, Y.C. Kim, K.B. Kim, H.K. Seok, E. Fleury, Sci. Tech. Adv. Mater. 6 (2005) 282–289.
[5] E.A. Cho, U.-S. Jeon, H.Y. Ha, S.-A. Hong, I.-H. OH, J. Power Sources 125 (2004) 178–182.
[6] R.L. Borup, N.E. Vanderburgh, Design and testing criteria for bipolar plate materials for PEM fuel cell applications, in: D.H. Doughty, B. Vyas, J.R. Huff, T. Takawara (Eds.), Proc. Mater. Res. Soc. Symp. 393 (1995) 151.
[7] H. Wang, M.A. Sweikart, J.A. Turner, J. Power Sources 115 (2003) 243–251.
[8] K. Shirakawa, K. Fukamichi, T. Kaneko, T. Masumoto, J. Phys. F: Met. Phys. 14 (1984) 1491–1499.
[9] C.M.A. Brett, A.M. Brett, Electrochemistry: Principles, Methods and Application, Oxford University Press, 1998.
[10] A.J. Sedriks, Corrosion of Stainless steel, John Wiley & Sons, New York, 1979.
[11] J. Jayaraj, K.B. Kim, H.S. Ahn, E. Fleury, Mater. Sci. Eng. A, in press.
[12] A. Inoue, Acta Mater. 48 (2000) 279–306.
[13] Y. Kawamura, T. Itoi, T. Nakamura, A. Inoue, Mater. Sci. Eng. A. 304 (2001) 735–739.
[14] A. Inoue, T. Shimizu, S. Yamaura, Y. Fujita, Mater. Trans. 46 (2005) 1706–1710.